

Synthesis, Structural Characterization, Ligand Displacement Reaction, and Electrochemical Property of Ruthenium Complexes Incorporating Linked Cyclopentadienyl-Carboranyl Ligands

Yi Sun,[†] Hoi-Shan Chan,[†] Pierre H. Dixneuf,[‡] and Zuowei Xie^{*,†}

Department of Chemistry, The Chinese University of Hong Kong, Shatin, New Territories, Hong Kong, China, and Institut de Chimie de Rennes, UMR 6509 CNRS, Université de Rennes, Organométalliques et Catalyse, Campus de Beaulieu, 35042 Rennes, France

Received August 10, 2004

Reactions of the dilithium salts of carbon-bridged cyclopentadienyl-carboranyl ligands with 1 equiv of $[\text{RuCl}_2(\text{COD})]_x$ in THF afforded the organoruthenium(II) complexes $[\eta^5\text{-}\sigma\text{-Me}_2\text{C}(\text{C}_5\text{H}_4)(\text{C}_2\text{B}_{10}\text{H}_{10})]\text{Ru}(\text{COD})$ (**1a**), $[\eta^5\text{-}\sigma\text{-Me}_2\text{C}(\text{C}_9\text{H}_6)(\text{C}_2\text{B}_{10}\text{H}_{10})]\text{Ru}(\text{COD})$ (**2a**), and $[\eta^5\text{-}\sigma\text{-H}_2\text{C}(\text{C}_{13}\text{H}_8)(\text{C}_2\text{B}_{10}\text{H}_{10})]\text{Ru}(\text{COD})$ (**3a**), respectively. Treatment of **1a** with bidentate tertiary phosphines in THF gave the corresponding COD displacement complexes $[\eta^5\text{-}\sigma\text{-Me}_2\text{C}(\text{C}_5\text{H}_4)(\text{C}_2\text{B}_{10}\text{H}_{10})]\text{Ru}(\text{dppe})$ (**1b**, dppe = 1,2-bis(diphenylphosphino)ethane), $[\eta^5\text{-}\sigma\text{-Me}_2\text{C}(\text{C}_5\text{H}_4)(\text{C}_2\text{B}_{10}\text{H}_{10})]\text{Ru}(\text{dppm})$ (**1c**, dppm = bis(diphenylphosphino)methane), $[\eta^5\text{-}\sigma\text{-Me}_2\text{C}(\text{C}_5\text{H}_4)(\text{C}_2\text{B}_{10}\text{H}_{10})]\text{Ru}(\text{dppf})$ (**1d**, dppf = 1,1'-bis(diphenylphosphino)ferrocene), and $[\eta^5\text{-}\sigma\text{-Me}_2\text{C}(\text{C}_5\text{H}_4)(\text{C}_2\text{B}_{10}\text{H}_{10})]\text{Ru}(\text{dppc})$ (**1e**, dppc = 1,2-(Ph₂P)₂-1,2-C₂B₁₀H₁₀). **1a** also reacted with 2,2'-bipyridine (bipy) to offer $[\eta^5\text{-}\sigma\text{-Me}_2\text{C}(\text{C}_5\text{H}_4)(\text{C}_2\text{B}_{10}\text{H}_{10})]\text{Ru}(\text{bipy})$ (**1f**). However, **1a** did not react with monodentate tertiary phosphines such as PPh₃ and PCy₃, tertiary amines, and bidentate ligands with no π -acidity such as dimethoxyethane and tetramethylethylenediamine. These results imply that a bidentate ligand with π -acidity is critical to displace the COD in **1a**. The electrochemical studies showed that the electron-donating power of various ligands increases in the following order: cyclopentadienyl < indenyl < fluorenyl, and COD < dppc < dppm \approx dppe < bipy. All of these new complexes were fully characterized by various spectroscopic techniques and elemental analyses. Their molecular structures (except for **1d**) were further confirmed by single-crystal X-ray analyses.

Introduction

Ruthenium half-sandwich complexes of the type $(\eta^5\text{-C}_5\text{R}_5)\text{RuXL}_2$ [R = H, Me; X = Cl, Br; L₂ = phosphines, COD (1,5-cyclooctadiene)] are effective catalysts for C–C bond-forming reactions.¹ For example, $(\eta^5\text{-C}_5\text{H}_5)\text{RuCl}(\text{COD})$ catalyzed a variety of coupling reactions of C \equiv C and C=C bonds for the production of functional dienes.² $(\eta^5\text{-C}_5\text{Me}_5)\text{RuCl}(\text{COD})$ allowed the head-to-head coupling of alkynes to form dienes and cyclobutenes³ or the sequential coupling of alkynes generating aromatic compounds.⁴ $(\eta^5\text{-C}_5\text{Me}_5)\text{RuCl}(\text{COD})$ also promoted double addition of carbene to alkynes and to enynes to generate dienes and bicyclo[3.1.0]hexane derivatives.⁵ The success of these catalytic processes is attributed to the

electron richness of the metal center and to the labile ligands, thus favoring oxidative coupling of the unsaturated molecules, and to the steric hindrance of the C₅-Me₅ group favoring regioselective couplings.¹ By contrast, $(\eta^5\text{-C}_5\text{R}_5)\text{RuCl}(\text{PPh}_3)_2$ complexes underwent activation of terminal alkynes into ruthenium-vinylidene key intermediates that controlled catalytic anti-Markovnikov additions to alkynes.⁶ These catalytic processes are favored by electron-releasing PR₃ ligands and illustrate how simple COD/ligand exchanges can modify the action of the catalyst.

On the other hand, ruthenium half-sandwich complexes, in which a cyclopentadienyl ligand is tethered to a donor atom, also receive much attention.⁷ The tethered donor atom in Cp-D chelating ligands can prevent rotation of the Cp ring and allow the planar chirality to be exploited in an efficient discrimination, through a strong coordination to the Ru atom, or can temporarily and reversibly coordinate to a Ru atom while stabilizing highly reactive, electronically and sterically unsaturated species,⁸ to meet the requirements of various catalytic processes. For example, a

* To whom correspondence should be addressed. Fax: (852)-26035057. Tel: (852)26096269. E-mail: zxie@cuhk.edu.hk.

[†] The Chinese University of Hong Kong.

[‡] Université de Rennes.

(1) (a) Trost, B. M.; Toste, F. D.; Pinkerton, A. B. *Chem. Rev.* **2001**, *101*, 2067. (b) Dérien, S.; Dixneuf, P. H. *J. Organomet. Chem.* **2004**, *689*, 1382.

(2) Trost, B. M. *Acc. Chem. Res.* **2002**, *35*, 695.

(3) (a) Paih, J. Le.; Monnier, F.; Dérien, S.; Dixneuf, P. H.; Clot, E.; Eisenstein, O. *J. Am. Chem. Soc.* **2003**, *125*, 11964. (b) Paih, J. Le.; Dérien, S.; Bruneau, C.; Demerseman, B.; Toupet, L.; Dixneuf, P. H. *Angew. Chem., Int. Ed.* **2001**, *40*, 2912.

(4) Yamamoto, Y.; Ogawa, R.; Itoh, K. *Chem. Commun.* **2000**, 549.

(5) (a) Paih, J. Le.; Dérien, S.; Özdemir, I.; Dixneuf, P. H. *J. Am. Chem. Soc.* **2000**, *122*, 7400. (b) Monnier, F.; Castillo, D.; Dérien, S.; Toupet, L.; Dixneuf, P. H. *Angew. Chem., Int. Ed.* **2003**, *42*, 5474.

(6) (a) Bruneau, C.; Dixneuf, P. H. *Acc. Chem. Res.* **1999**, *32*, 311.

(b) Trost, B. M.; Martinez, J. A.; Kulawiec, R. J.; Indolese, A. F. *J. Am. Chem. Soc.* **1993**, *115*, 10402. (c) Jérôme, F.; Monnier, F.; Lawicka, H.; Dérien, S.; Dixneuf, P. H. *Chem. Commun.* **2003**, 696.

(7) Jutzi, P.; Redeker, T. *Eur. J. Inorg. Chem.* **1998**, 663.

(8) Ganter, C. *Chem. Soc. Rev.* **2003**, *32*, 130.

phosphine-tethered Cp ligand was used in the reconstitutive addition of alkynes and allyl alcohols,⁹ since a rigid (Cp-PPh₂)Ru⁺ moiety was required in catalysis. In contrast, a hemilabile amido-appended Cp ligand was employed in direct derivatization of peptides and proteins¹⁰ or proton transfer reactions.¹¹ In the case where a substrate is more coordinating than the tethered donor atom, the functionalized side-arm will lose its function as a coordinating unit, which in turn will change the properties of the resulting Ru catalysts. To solve this problem, a new bidentate ligand system is desired.

We have recently developed a novel class of linked cyclopentadienyl-carboranyl ligands which are finding many applications in rare earth and early transition metal chemistry.¹² Recent work showed that the [η^5 : σ -Me₂C(C₅H₄)(C₂B₁₀H₁₀)]M (M = Ti, Zr, Hf) moiety remains intact in ethylene polymerization and multiple insertion reactions of unsaturated molecules due to the presence of the sterically bulky carboranyl unit.¹³ It is anticipated that the [η^5 : σ -Me₂C(C₅H₄)(C₂B₁₀H₁₀)]Ru moiety will be stable and remain intact in catalysis and the electronic property of the metal center should be tunable by variation of the structures of the π ligands. It is hoped that the rigidity of this type of ligand and unique property of the carborane molecule would add some new features to organoruthenium chemistry, especially as the σ (alkyl) carbon–ruthenium bond in such systems is not stable via either β elimination or insertion reaction. With this in mind, we have extended our research to include the late transition metals and report herein the syntheses, X-ray structures, and electrochemical properties of [η^5 : σ -R₂C(L)(C₂B₁₀H₁₀)]Ru(COD) (R = CH₃, L = C₅H₄, C₉H₆; R = H, L = C₁₃H₈) and their phosphines derivatives generated from COD displacement reactions.

Experimental Section

General Procedures. All experiments were performed under an atmosphere of dry dinitrogen with the rigid exclusion of air and moisture using standard Schlenk or cannula techniques, or in a glovebox. THF and *n*-hexane were freshly distilled from sodium benzophenone ketyl immediately prior to use. CH₂Cl₂ was freshly distilled from CaH₂ and P₂O₅, respectively, immediately prior to use. Me₂C(C₅H₅)(C₂B₁₀H₁₁),¹⁴ Me₂C(C₉H₇)(C₂B₁₀H₁₁),¹⁵ dibenzofulvene,¹⁶ 6,6'-dimethyldibenzofulvene,¹⁷ [RuCl₂(COD)]_x,¹⁸ 1,2-(Ph₂P)₂-1,2-C₂B₁₀H₁₀,¹⁹ and

1,1'-bis(diphenylphosphino)ferrocene²⁰ were prepared according to literature methods. All other chemicals were purchased from either Aldrich or Acros Chemical Co. and used as received unless otherwise noted. Cyclic voltammetric measurements were performed using a BAS CV-50W voltammetric analyzer. The electrochemical cell comprised a platinum-wire working electrode, a silver-wire reference electrode, and a platinum-disk counter electrode. All measurements were made in a dry N₂ atmosphere. All sample solutions (CH₂Cl₂) contained *n*-Bu₄NPF₆ (0.15 M) as supporting electrolyte and complex (2.0 × 10⁻³ M). Chemical potentials were internally referenced to the ferrocenium/ferrocene redox system. Infrared spectra were obtained from KBr pellets prepared in the glovebox on a Perkin-Elmer 1600 Fourier transform spectrometer. ¹H and ¹³C NMR spectra were recorded on a Bruker DPX 300 spectrometer at 300 and 75 MHz, respectively. ¹¹B and ³¹P NMR spectra were recorded on a Varian Inova 400 spectrometer at 128 and 162 MHz, respectively. All chemical shifts are reported in δ units with references to the residual protons of the deuterated solvents for proton and carbon chemical shifts, to external BF₃·OEt₂ (0.0 ppm) for boron chemical shifts, and to external 85% H₃PO₄ (0.0 ppm) for phosphorus chemical shifts. Mass spectra were recorded on a Thermo Finnigan MAT 95 XL spectrometer. Elemental analyses were performed by either MEDAC Ltd. U.K. or Shanghai Institute of Organic Chemistry, CAS, China.

Preparation of H₂C(C₁₃H₉)(C₂B₁₀H₁₁) (3). To a solution of *o*-C₂B₁₀H₁₂ (1.00 g, 6.90 mmol) in a dry toluene/diethyl ether (2:1, 15 mL) mixture was added dropwise a 1.60 M solution of *n*-BuLi in *n*-hexane (8.70 mL, 13.90 mmol) at -78 °C with stirring, and the mixture was warmed to room temperature and stirred for 3 h. This solution was then cooled to 0 °C, and a solution of dibenzofulvene (2.45 g, 13.80 mmol) in a toluene/diethyl ether (2:1, 15 mL) mixture was slowly added. The reaction mixture was stirred at 80 °C overnight, quenched with 20 mL of a saturated NH₄Cl aqueous solution at 0 °C, transferred to a separatory funnel, and then diluted with 30 mL of diethyl ether. The organic layer was separated, and the aqueous layer was extracted with Et₂O (3 × 15 mL). The combined ether solutions were dried over anhydrous MgSO₄ and concentrated to give a crude yellow solid, which was purified by column chromatography (SiO₂, hexane/ether, 4:1) to yield **3** as pale yellow crystals (1.90 g, 85%). ¹H NMR (300 MHz, CDCl₃): δ 7.75 (d, *J* = 6.9 Hz, 2H, aryl H), 7.52 (d, *J* = 7.5 Hz, 2H, aryl H), 7.44–7.33 (m, 4H, aryl H), 4.12 (t, *J* = 4.5 Hz, 1H, sp³-CH in fluorenyl), 3.46 (s, 1H, CH of cage), 3.05 (d, *J* = 4.5 Hz, 2H, CH₂). ¹³C NMR (75 MHz, CDCl₃): δ 145.9, 141.3, 128.5, 128.3, 124.8, 120.9 (aryl C), 75.3, 61.8 (cage C), 47.8 (sp³-C in fluorenyl), 42.2 (CH₂). ¹¹B NMR (128 MHz, CDCl₃): δ -2.1 (1B), -5.4 (1B), -9.3 (2B), -11.1 (2B), -11.8 (2B), -12.9 (2B). IR (KBr, cm⁻¹): ν_{BH} 2574 (vs). Anal. Calcd for C₁₆H₂₂B₁₀: C, 59.60; H, 6.88. Found: C, 60.27; H, 6.82. HR-FABMS: *m/z* calcd for C₁₆H₂₂B₁₀, 322.2719; found, 322.2726.

Preparation of [η^5 : σ -Me₂C(C₅H₄)(C₂B₁₀H₁₀)]Ru(COD) (1a). A 1.60 M solution of *n*-BuLi in *n*-hexane (1.25 mL, 2.00 mmol) was slowly added to a THF solution (15 mL) of Me₂C-(C₅H₅)(C₂B₁₀H₁₁) (**1**; 0.25 g, 1.00 mmol) at -78 °C with stirring, and the mixture was warmed to room temperature and stirred overnight. The powder of [RuCl₂(COD)]_x (0.28 g, 1.00 mmol) was added to the resulting solution, and the mixture was stirred at room temperature for 48 h. After removal of the solvent and addition of CH₂Cl₂ (20 mL), the precipitate was filtered off, and the clear solution was concentrated to about 10 mL. **1a** was obtained as orange crystals after slow evaporation of the solvent (0.38 g, 82%). ¹H NMR (300 MHz, CDCl₃): δ 5.07 (m, 2H, C₅H₄), 4.79 (m, 2H, CH of COD), 4.57 (m, 2H, C₅H₄), 3.68 (m, 2H, CH of COD), 2.63 (m, 2H, CH₂ of COD), 2.02 (m, 4H, CH₂ of COD), 1.76 (m, 2H, CH₂ of COD), 1.38 (s,

(9) Trost, B. M.; Vidal, B.; Thommen, M. *Chem. Eur. J.* **1999**, *5*, 1055.

(10) Grotjahn, D. B.; Joubran, C.; Combs, D.; Brune, D. C. *J. Am. Chem. Soc.* **1998**, *120*, 11814.

(11) (a) Ayllon, J. A.; Sayers, S. F.; Sabo-Etienne, S.; Donnadieu, B.; Chaudret, B.; Clot, E. *Organometallics* **1999**, *18*, 3981. (b) Chu, H. S.; Lau, C. P.; Wong, K. Y. *Organometallics* **1998**, *17*, 2768.

(12) Xie, Z. *Acc. Chem. Res.* **2003**, *36*, 1.

(13) (a) Wang, H.; Wang, Y.; Li, H.-W.; Xie, Z. *Organometallics* **2001**, *20*, 5110. (b) Wang, H.; Li, H.-W.; Xie, Z. *Organometallics* **2003**, *22*, 4522. (c) Wang, Y.; Wang, H.; Wang, H.; Chan, H.-S.; Xie, Z. *J. Organomet. Chem.* **2003**, *683*, 39. (d) Wang, J.; Zheng, C.; Maguire, J. A.; Hosmane, N. S. *Organometallics* **2003**, *22*, 4839.

(14) Chui, K.; Yang, Q.; Mak, T. C. W.; Xie, Z. *Organometallics* **2000**, *19*, 1391.

(15) Wang, S.; Yang, Q.; Mak, T. C. W.; Xie, Z. *Organometallics* **2000**, *19*, 334.

(16) Nakano, T.; Takewaki, K.; Yade, T.; Okamoto, Y. *J. Am. Chem. Soc.* **2001**, *123*, 9182.

(17) Kice, J. L. *J. Am. Chem. Soc.* **1958**, *80*, 348.

(18) Albers, M. O.; Ashworth, T. V.; Oosthuizen, H. E.; Singleton, E. *Inorg. Synth.* **1989**, *26*, 68.

(19) Alexander, R. P.; Schroeder, H. *Inorg. Chem.* **1963**, *2*, 1107.

(20) Bishop, J. J.; Davison, A.; Katcher, M. L.; Lichtenberg, D. W.; Merrill, R. E.; Smart, J. C. *J. Organomet. Chem.* **1971**, *27*, 241.

6H, C(CH₃)₂). ¹³C NMR (75 MHz, CDCl₃): δ 87.8, 86.4 (C₅H₄), 74.8, 74.7 (CH of COD), 39.8 (C(CH₃)₂), 33.1, 28.1 (CH₂ of COD), 31.9 (CH₃). ¹¹B NMR (128 MHz, CDCl₃): δ -4.3 (1B), -5.1 (1B), -6.6 (2B), -8.9 (4B), -9.8 (2B). IR (KBr, cm⁻¹): ν_{BH} 2570 (vs). Anal. Calcd for C₁₈H₃₂B₁₀Ru: C, 47.24; H, 7.05. Found: C, 46.82; H, 6.88.

Preparation of [η⁵:σ-Me₂C(C₅H₆)(C₂B₁₀H₁₀)]Ru(COD) (2a). This complex was prepared as red-brown crystals from *n*-BuLi in *n*-hexane (1.60 M, 1.25 mL, 2.00 mmol), Me₂C(C₉H₇)-(C₂B₁₀H₁₁) (2; 0.30 g, 1.00 mmol), and [RuCl₂(COD)]_x (0.28 g, 1.00 mmol) in THF (15 mL) using the identical procedures reported for **1a**: yield 0.33 g (64%). ¹H NMR (300 MHz, CDCl₃): δ 7.76 (d, *J* = 8.7 Hz, 1H, aryl H), 7.39 (dd, *J* = 8.7 and 6.6 Hz, 1H, aryl H), 7.11 (d, *J* = 8.7 Hz, 1H, aryl H), 6.91 (dd, *J* = 8.7 and 6.6 Hz, 1H, aryl H), 5.60 (d, *J* = 2.7 Hz, 1H, indenyl), 4.80 (d, *J* = 2.7 Hz, 1H, indenyl), 4.62 (m, 1H, CH of COD), 3.70 (m, 1H, CH of COD), 2.80 (m, 2H, CH of COD), 2.72 (m, 2H, CH₂ of COD), 2.50 (m, 2H, CH₂ of COD), 2.25 (m, 2H, CH₂ of COD), 1.86 (m, 2H, CH₂ of COD), 1.68 (s, 3H, C(CH₃)₂), 1.43 (s, 3H, C(CH₃)₂). ¹³C NMR (75 MHz, CDCl₃): δ 131.5, 129.7, 125.5, 123.2, 118.4, 112.7, 87.8, 84.3, 84.2 (indenyl), 82.0, 79.0, 77.2, 75.3 (CH of COD), 42.7 (C(CH₃)₂), 38.0, 27.6, 27.4, 26.3 (CH₂ of COD), 33.7, 32.7 (CH₃). ¹¹B NMR (128 MHz, CDCl₃): δ -3.8 (1B), -4.3 (1B), -6.5 (2B), -9.1 (6B). IR (KBr, cm⁻¹): ν_{BH} 2570 (vs). Anal. Calcd for C₂₂H₃₄B₁₀-Ru: C, 52.04; H, 6.75. Found: C, 51.76; H, 6.56.

Preparation of [η⁵:σ-H₂C(C₁₃H₈)(C₂B₁₀H₁₀)]Ru(COD) (3a). This complex was prepared as dark red crystals from *n*-BuLi in *n*-hexane (1.60 M, 1.25 mL, 2.00 mmol), H₂C(C₁₃H₉)-(C₂B₁₀H₁₁) (3; 0.32 g, 1.00 mmol), and [RuCl₂(COD)]_x (0.28 g, 1.00 mmol) in THF (15 mL) using the identical procedures reported for **1a**: yield 0.28 g (52%). ¹H NMR (300 MHz, C₆D₆): δ 7.06–6.88 (m, 4H, aryl H), 6.89 (d, *J* = 8.7 Hz, 2H, aryl H), 6.49 (dd, *J* = 8.7 and 6.3 Hz, 2H, aryl H), 3.33 (d, *J* = 5.7 Hz, 2H, CH₂), 3.10 (m, 4H, CH of COD), 2.32 (m, 4H, CH₂ of COD), 1.71 (m, 4H, CH₂ of COD). ¹³C NMR (75 MHz, C₆D₆): δ 156.5, 130.7, 127.5, 127.2, 126.8, 126.5, 125.6, 124.5, 124.2, 120.4, 119.9, 119.2, 109.4 (aryl C), 88.8, 77.5, 68.2, 65.1 (CH of COD), 45.9 (CH₂), 35.8, 31.0, 28.7, 25.1 (CH₂ of COD). ¹¹B NMR (128 MHz, C₆D₆): δ -2.8 (2B), -5.5 (4B), -8.1 (4B). IR (KBr, cm⁻¹): ν_{BH} 2550 (vs). Anal. Calcd for C₂₂H₃₄B₁₀Ru: C, 52.04; H, 6.75. Found: C, 52.00; H, 6.55.

Preparation of [η⁵:σ-Me₂C(C₅H₄)(C₂B₁₀H₁₀)]Ru(dppe) (1b). A THF solution (10 mL) of [η⁵:σ-Me₂C(C₅H₄)(C₂B₁₀H₁₀)]-Ru(COD) (**1a**; 0.23 g, 0.50 mmol) and a THF solution (5 mL) of dppe (0.24 g, 0.60 mmol) were mixed at room temperature and stirred for 24 h. After removal of THF, the resulting solid was washed with *n*-hexane. Recrystallization from CH₂Cl₂ (10 mL) gave **1b** as yellow crystals (0.30 g, 81%). ¹H NMR (300 MHz, CDCl₃): δ 7.92–6.74 (m, 20H, aryl H), 5.32 (m, 2H, C₅H₄), 4.30 (m, 2H, C₅H₄), 2.87 (t, *J* = 9.0 Hz, 2H, CH₂), 2.48 (t, *J* = 9.0 Hz, 2H, CH₂), 1.48 (s, 6H, CH₃). ¹³C NMR (75 MHz, CDCl₃): δ 132.4, 131.6, 130.8, 129.5, 128.9, 128.4, 128.0, 127.6 (aryl C), 82.7, 74.6 (C₅H₄), 39.8 (C(CH₃)₂), 31.6 (CH₃), 24.6 (d, *J*_{CP} = 21.2 Hz, PCH₂CH₂P). ¹¹B NMR (128 MHz, CDCl₃): δ -4.2 (2B), -7.5 (4B), -9.6 (4B). ³¹P NMR (162 MHz, CDCl₃): δ 81.03. IR (KBr, cm⁻¹): ν_{BH} 2563 (s). Anal. Calcd for C₃₆H₄₄B₁₀P₂Ru: C, 57.82; H, 5.93. Found: C, 57.70; H, 5.79.

Preparation of [η⁵:σ-Me₂C(C₅H₄)(C₂B₁₀H₁₀)]Ru(dppm) (1c). A THF solution (10 mL) of [η⁵:σ-Me₂C(C₅H₄)(C₂B₁₀H₁₀)]-Ru(COD) (**1a**; 0.23 g, 0.50 mmol) and a THF solution (5 mL) of dppm (0.23 g, 0.60 mmol) were mixed at room temperature and then refluxed for 24 h, followed by the identical procedures reported for **1b** to give **1c** as yellow crystals (0.28 g, 75%). ¹H NMR (300 MHz, CDCl₃): δ 7.67–6.99 (m, 20H, aryl H), 5.30 (m, 2H, C₅H₄), 5.06 (m, 1H, PCH₂P), 4.38 (m, 2H, C₅H₄), 4.01 (m, 1H, PCH₂P), 1.60 (s, 6H, CH₃). ¹³C NMR (75 MHz, CDCl₃): δ 139.0, 133.9, 131.7, 131.2, 129.9, 129.2, 128.7, 128.0 (aryl C), 81.0, 71.3 (C₅H₄), 43.90 (PCH₂P), 40.1 (C(CH₃)₂), 32.1 (CH₃). ¹¹B NMR (128 MHz, CDCl₃): δ -4.0 (2B), -7.0 (4B), -9.2 (4B). ³¹P NMR (162 MHz, CDCl₃): δ 13.23. IR (KBr,

cm⁻¹): ν_{BH} 2578 (vs). Anal. Calcd for C₃₅H₄₂B₁₀P₂Ru: C, 57.28; H, 5.77. Found: C, 57.55; H, 5.94.

Preparation of [η⁵:σ-Me₂C(C₅H₄)(C₂B₁₀H₁₀)]Ru(dppf) (1d). A THF solution (10 mL) of [η⁵:σ-Me₂C(C₅H₄)(C₂B₁₀H₁₀)]-Ru(COD) (**1a**; 0.23 g, 0.50 mmol) and a THF solution (5 mL) of dppf (0.31 g, 0.60 mmol) were mixed at room temperature and then refluxed for 24 h, followed by the identical procedures reported for **1b** to give **1d** as yellow solids (0.38 g, 84%). ¹H NMR (300 MHz, CDCl₃): δ 7.61–7.29 (m, 20H, aryl H), 4.98, 4.46, 4.34, 4.29, 4.19, 3.88 (br, 2H each, C₅H₄), 1.38 (s, 6H, CH₃). ¹³C NMR (75 MHz, CDCl₃): δ 135.3, 134.8, 131.5, 129.9, 129.7, 127.6 (aryl C), 81.9, 76.6, 75.6, 74.9, 71.4, 70.6 (C₅H₄), 40.2 (C(CH₃)₂), 32.1 (CH₃). ¹¹B NMR (128 MHz, CDCl₃): δ -3.7 (2B), -6.5 (8B). ³¹P NMR (162 MHz, CDCl₃): δ 41.47. IR (KBr, cm⁻¹): ν_{BH} 2545 (vs). Anal. Calcd for C₄₄H₄₈B₁₀FeP₂Ru: C, 58.47; H, 5.36. Found: C, 58.70; H, 5.37.

Preparation of [η⁵:σ-Me₂C(C₅H₄)(C₂B₁₀H₁₀)]Ru(dppe)·THF (1e·THF). A THF solution (10 mL) of [η⁵:σ-Me₂C(C₅H₄)-(C₂B₁₀H₁₀)]Ru(COD) (**1a**; 0.23 g, 0.50 mmol) and a THF solution (5 mL) of dppe (1,2-(Ph₂P)₂-1,2-C₂B₁₀H₁₀) (0.31 g, 0.60 mmol) were mixed at room temperature and then refluxed for 48 h, followed by the identical procedures reported for **1b** to give **1e**·THF as yellow crystals (0.64 g, 68%). ¹H NMR (300 MHz, CDCl₃): δ 8.00–7.00 (m, 20H, aryl H), 4.64 (m, 2H, C₅H₄), 4.26 (m, 2H, C₅H₄), 3.63 (m, 4H, THF), 1.61 (m, 4H, THF), 1.32 (s, 6H, CH₃). ¹³C NMR (75 MHz, CDCl₃): δ 136.6, 136.4, 136.2, 135.6, 131.2, 129.0, 127.4 (aryl C), 90.5, 90.2, 88.3 (C₅H₄), 39.7 (C(CH₃)₂), 32.0 (CH₃). ¹¹B NMR (128 MHz, CDCl₃): δ -3.6 (6B), -5.9 (2B), -8.4 (12B). ³¹P NMR (162 MHz, CDCl₃): δ 99.84. IR (KBr, cm⁻¹): ν_{BH} 2566 (s). Anal. Calcd for C₄₀H₅₈B₂₀OP₂Ru: C, 51.43; H, 6.26. Found: C, 51.48; H, 5.96.

Preparation of [η⁵:σ-Me₂C(C₅H₄)(C₂B₁₀H₁₀)]Ru(bipy) (1f). A toluene solution (10 mL) of [η⁵:σ-Me₂C(C₅H₄)(C₂B₁₀H₁₀)]-Ru(COD) (**1a**; 0.23 g, 0.50 mmol) and a THF solution (5 mL) of 2,2'-bipyridine (0.08 g, 0.50 mmol) were mixed at room temperature and then refluxed for 48 h, followed by the identical procedures reported for **1b** to give **1f** as purple crystals (0.18 g, 71%). ¹H NMR (300 MHz, CDCl₃): δ 9.37 (d, *J* = 5.4 Hz, 2H, bipy), 8.03 (d, *J* = 8.1 Hz, 2H, bipy), 7.66 (dd, *J* = 8.1 and 7.6 Hz, 2H, bipy), 7.27 (dd, *J* = 7.6 and 5.4 Hz, 2H, bipy), 4.41 (m, 2H, C₅H₄), 3.99 (m, 2H, C₅H₄), 1.59 (s, 6H, CH₃). ¹³C NMR (75 MHz, CDCl₃): δ 153.8, 132.5, 124.4, 122.0 (bipy), 80.1, 77.2 (C₅H₄), 41.7 (C(CH₃)₂), 31.9 (CH₃). ¹¹B NMR (128 MHz, CDCl₃): δ -3.1 (1B), -3.8 (1B), -5.2 (1B), -7.5 (2B), -8.5 (2B), -10.2 (1B), -12.7 (2B). IR (KBr, cm⁻¹): ν_{BH} 2570 (vs). Anal. Calcd for C₂₀H₂₈B₁₀N₂Ru: C, 47.51; H, 5.58; N, 5.54. Found: C, 47.60; H, 5.60; N, 5.60.

X-ray Structure Determination. All single crystals were immersed in Paratone-N oil and sealed under N₂ in thin-walled glass capillaries. Data were collected at 293 K on a Bruker SMART 1000 CCD diffractometer using Mo Kα radiation. An empirical absorption correction was applied using the SADABS program.²¹ All structures were solved by direct methods and subsequent Fourier difference techniques and refined anisotropically for all non-hydrogen atoms by full-matrix least squares calculations on *F*² using the SHELXTL program package.^{22a} For noncentrosymmetric structure **1b**, the appropriate enantiomorph was chosen by refining Flack's parameter *x* toward zero.^{22b} Most of the carborane hydrogen atoms were located from difference Fourier syntheses. All other hydrogen atoms were geometrically fixed using the riding model. Crystal data and details of data collection and structure

(21) Sheldrick, G. M. *SADABS*, Program for Empirical Absorption Correction of Area Detector Data; University of Göttingen: Germany, 1996.

(22) (a) Sheldrick, G. M. *SHELXTL 5.10* for Windows NT: Structure Determination Software Programs; Bruker Analytical X-ray Systems, Inc.: Madison, WI, 1997. (b) Flack, H. D. *Acta Crystallogr.* **1983**, A39, 876.

Table 1. Crystal Data and Summary of Data Collection and Refinement for 1a–3a and 3

	1a	2a	3a	3
formula	C ₁₈ H ₃₂ B ₁₀ Ru	C ₂₂ H ₃₄ B ₁₀ Ru	C ₂₄ H ₃₂ B ₁₀ Ru	C ₁₆ H ₂₂ B ₁₀
cryst size (mm)	0.80 × 0.55 × 0.40	0.60 × 0.40 × 0.15	0.40 × 0.35 × 0.30	0.30 × 0.25 × 0.20
fw	457.6	507.7	529.7	322.4
cryst syst	triclinic	monoclinic	orthorhombic	monoclinic
space group	<i>P</i> 1	<i>Cc</i>	<i>Pnma</i>	<i>P</i> 2 ₁ / <i>c</i>
<i>a</i> , Å	9.236(1)	7.278(1)	10.219(2)	11.681(2)
<i>b</i> , Å	10.181(1)	21.082(2)	11.867(2)	23.528(5)
<i>c</i> , Å	12.537(1)	15.304(2)	20.697(4)	13.623(3)
α, deg	86.31(1)	90	90	90
β, deg	74.17(1)	98.88(1)	90	90
γ, deg	69.23(1)	90	90	90
<i>V</i> , Å ³	1059.9(1)	2320.0(4)	2509.8(9)	3744(1)
<i>Z</i>	2	4	4	8
<i>D</i> _{calcd} , Mg/m ³	1.434	1.453	1.402	1.144
radiation (λ) Å	Mo Kα (0.71073)	Mo Kα (0.71073)	Mo Kα (0.71073)	Mo Kα (0.71073)
2θ _{max} , deg	56.0	56.0	51.0	50.0
μ, mm ^{−1}	0.742	0.686	0.638	0.056
<i>F</i> (000)	468	1040	1080	1344
no. of obsd rflns	5002	4765	2214	4296
no. of params refnd	262	299	170	471
goodness of fit	1.113	1.061	1.175	1.046
<i>R</i> 1	0.061	0.057	0.039	0.084
<i>wR</i> 2	0.175	0.134	0.111	0.259

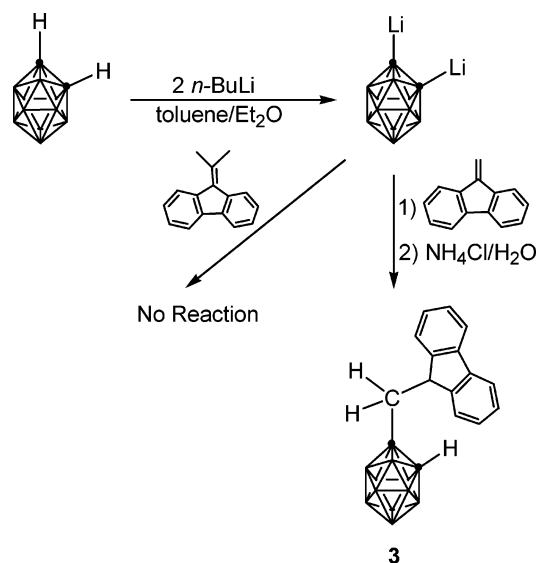
Table 2. Crystal Data and Summary of Data Collection and Refinement for 1b, 1c, 1e, and 1f

	1b	1c	1e·THF	1f
formula	C ₃₆ H ₄₄ B ₁₀ P ₂ Ru	C ₃₅ H ₄₂ B ₁₀ P ₂ Ru	C ₄₀ H ₅₈ B ₂₀ OP ₂ Ru	C ₂₀ H ₂₈ B ₁₀ N ₂ Ru
cryst size (mm)	0.20 × 0.10 × 0.05	0.40 × 0.30 × 0.20	0.20 × 0.10 × 0.05	0.40 × 0.30 × 0.20
fw	747.8	733.8	934.1	505.6
cryst syst	monoclinic	monoclinic	monoclinic	triclinic
space group	<i>P</i> 2 ₁	<i>P</i> 2 ₁ / <i>c</i>	<i>P</i> 2 ₁ / <i>n</i>	<i>P</i> 1
<i>a</i> , Å	9.142(1)	9.167(1)	11.303(1)	9.142(1)
<i>b</i> , Å	17.669(1)	18.141(1)	31.324(2)	9.550(1)
<i>c</i> , Å	11.253(1)	21.169(1)	13.287(1)	14.199(2)
α, deg	90	90	90	105.91(1)
β, deg	91.48(1)	95.09(1)	96.93(1)	91.42(1)
γ, deg	90	90	90	102.02(1)
<i>V</i> , Å ³	1817.2(1)	3506.7(3)	4669.9(4)	1161.5(2)
<i>Z</i>	2	4	4	2
<i>D</i> _{calcd} , Mg/m ³	1.367	1.390	1.329	1.446
radiation (λ), Å	Mo Kα (0.71073)	Mo Kα (0.71073)	Mo Kα (0.71073)	Mo Kα (0.71073)
2θ _{max} , deg	50.0	56.1	50.0	56.0
μ, mm ^{−1}	0.547	0.565	0.439	0.688
<i>F</i> (000)	768	1504	1920	512
no. of obsd rflns	5972	8468	8229	5472
no. of params refnd	442	433	577	298
goodness of fit	1.221	1.054	1.140	1.048
<i>R</i> 1	0.048	0.060	0.044	0.046
<i>wR</i> 2	0.111	0.126	0.111	0.106

refinements are given in Tables 1 and 2, respectively. Further details are included in the Supporting Information.

Results and Discussion

Ligand. One of the objectives of this work is to study the effects of the structures of π ligands on electron richness of the Ru metal center and on the molecular structures of the resulting Ru metal complexes. The C-bridged ligands, Me₂C(C₅H₅)(C₂B₁₀H₁₁) (**1**)¹⁴ and Me₂C-(C₉H₇)(C₂B₁₀H₁₁) (**2**)¹⁵ were developed earlier in our laboratory. We attempted to prepare the fluorenyl analogue, Me₂C(C₁₃H₉)(C₂B₁₀H₁₁), using the known procedures. However, 6,6'-dimethyldibenzofulvene did not react with Li₂C₂B₁₀H₁₀ under various reaction conditions because of steric reasons. A less bulkier substrate, dibenzofulvene, was then chosen instead. Treatment of Li₂C₂B₁₀H₁₀ with 2 equiv of dibenzofulvene in toluene/ether (2:1) gave, after hydrolysis with a saturated NH₄Cl aqueous solution, the desired product H₂C(C₁₃H₉)(C₂B₁₀H₁₁) (**3**) as pale yellow crystals in 85% isolated yield (Scheme 1). An excess amount of dibenzofulvene was necessary since part of it was polymerized under the reaction conditions.¹⁶

Scheme 1

The ¹H NMR spectrum of **3** showed multiplets of aromatic protons in the range 7.33–7.75 ppm, one

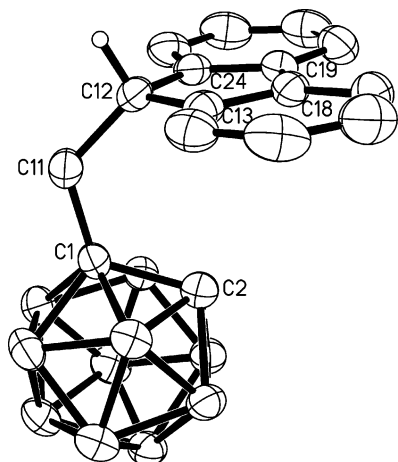


Figure 1. Molecular structure of $\text{H}_2\text{C}(\text{C}_{13}\text{H}_9)(\text{C}_2\text{B}_{10}\text{H}_{11})$ (**3**), showing one of the two independent molecules in the unit cell. Selected distances [Å] and angles [deg]: C1–C11 = 1.562(5) [1.529(5)], C11–C12 = 1.549(5) [1.546(5)], C1–C2 = 1.682(5) [1.652(5)], C12–C13 = 1.522(5) [1.520(5)], C12–C24 = 1.518(5) [1.519(5)], C1–C11–C12 = 121.6(3) [117.1(3)], C11–C12–C13 = 117.4(3) [113.2(3)], C11–C12–C24 = 117.5(3) [115.2(4)], C13–C12–C24 = 102.9(3) [102.5(3)]. Distances and angles in brackets are those of a second molecule.

triplet of the $\text{sp}^3\text{-CH}$ proton of the fluorenyl group at 4.12 ppm, one doublet of the bridging methylene protons at 3.05 ppm, and one singlet of the cage CH proton at 3.46 ppm. Its ^{13}C NMR spectrum exhibited six aromatic carbon signals, two cage carbon resonances, one methylene, and one $\text{sp}^3\text{-CH}$ carbon peak, respectively. The ^{11}B NMR spectrum displayed a 1:1:2:2:2 splitting pattern, which differed from that of compounds **1** (1:1:2:2:4) and **2** (1:1:3:2:3), respectively, indicating that the ^{11}B NMR spectra are very sensitive to the cage carbon substituents. The molecular structure of **3** was confirmed by an X-ray analysis and is shown in Figure 1. The bond distances and angles are normal in comparison with the literature data.¹²

$[\eta^5\text{-}\sigma\text{-R}_2\text{C}(\text{C}_5\text{R}'_4)(\text{C}_2\text{B}_{10}\text{H}_{10})]\text{Ru}(\text{COD})$ Complexes.

Compounds **1–3** contain two acidic protons, cage CH and $\text{sp}^3\text{-CH}$ of the cyclic group, which can be removed by strong bases such as *n*-BuLi to give the dianionic salts. Treatment of their dilithium salts with 1 equiv of $[\text{RuCl}_2(\text{COD})]_x$ at room temperature in THF afforded, respectively, $[\eta^5\text{-}\sigma\text{-Me}_2\text{C}(\text{C}_5\text{H}_4)(\text{C}_2\text{B}_{10}\text{H}_{10})]\text{Ru}(\text{COD})$ (**1a**) as orange crystals in 82% isolated yield, $[\eta^5\text{-}\sigma\text{-Me}_2\text{C}(\text{C}_9\text{H}_6)(\text{C}_2\text{B}_{10}\text{H}_{10})]\text{Ru}(\text{COD})$ (**2a**) as red crystals in 64% isolated yield, and $[\eta^5\text{-}\sigma\text{-H}_2\text{C}(\text{C}_{13}\text{H}_8)(\text{C}_2\text{B}_{10}\text{H}_{10})]\text{Ru}(\text{COD})$ (**3a**) as dark red crystals in 52% isolated yield (Scheme 2).

Complexes **1a–3a** are quite soluble in polar organic solvents such as THF and pyridine, soluble in toluene, CH_2Cl_2 , and CHCl_3 , but insoluble in *n*-hexane. Their stabilities in air follow the trend **1a** > **2a** > **3a**. **1a** is stable in air in both solid and solution phases. **2a** is stable in air in the solid state only, whereas **3a** is air-sensitive in both solid state and solution phase. The ^1H NMR spectra of **1a–3a** all showed the presence of the linked organic–inorganic hybrid ligand and COD in a molar ratio of 1:1. Their ^{13}C NMR spectra were in line with the ^1H NMR ones. The ^{11}B NMR spectra exhibited a 1:1:2:4:2 splitting pattern for **1a**, a 1:1:2:6 splitting pattern for **2a**, and a 2:4:4 splitting pattern for **3a**. Their

Scheme 2

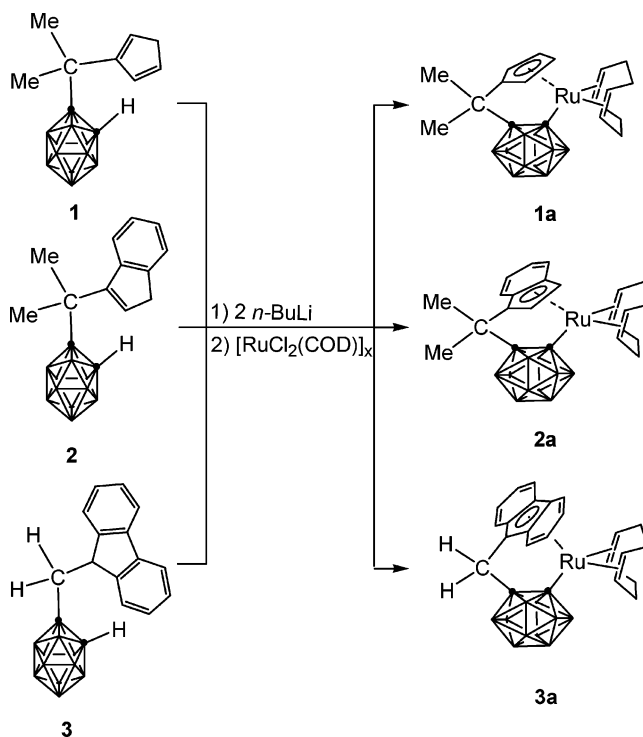


Table 3. Selected Structural Data for **1a–3a**^a

	1a	2a	3a
Ru–C _{cage}	2.213(3)	2.219(4)	2.228(4)
Ru–C _{ring}	2.207(3)	2.198(5)	2.202(4)
	2.222(4)	2.231(9)	2.344(3)
	2.227(4)	2.255(6)	2.344(3)
	2.238(4)	2.338(7)	2.449(3)
	2.256(4)	2.387(5)	2.449(3)
av Ru–C _{ring}	2.230(4)	2.282(9)	2.358(4)
av Ru–C _{COD}	2.238(4)	2.207(10)	2.185(4)
C=C (COD)	1.386(6)	1.383(10)	1.405(5)
	1.402(7)	1.400(9)	1.405(5)
av C=C (COD)	1.394(7)	1.3912(9)	1.405(5)
C _{ring} –C _{bridge} –C _{cage}	108.4(3)	108.3(4)	111.9(4)
Cent–Ru–C _{cage}	111.8	111.9	113.0

^a Cent: the centroid of the five-membered ring. Distances are in Å and angles are in deg.

solid-state IR spectra all displayed a characteristic terminal B–H absorption at $\sim 2550\text{ cm}^{-1}$.

The molecular structures of **1a–3a** were confirmed by single-crystal X-ray analyses and are shown in Figures 2–4, respectively. The coordination environments of the Ru atom in all three complexes are similar, in which the Ru(II) ion is η^5 -bonded to the five-membered ring of the cyclopentadienyl, or indenyl or fluorenyl group, σ -bound to the carborane cage carbon, and coordinated to two carbon–carbon double bonds of the COD molecule. Thus, they are 18-electron complexes. The selected bond distances and angles are compiled in Table 3 for comparison. The average Ru–C(C₅ ring) and C=C(COD) distances are in the order **1a** < **2a** < **3a**, whereas the average Ru–C(COD) distances get shorter from **1a** to **2a** to **3a**. These results indicate that the back-bonding between Ru(II) and COD becomes stronger from **1a** to **3a**, suggesting that the electron-donating power of π ligands follows the trend fluorenyl > indenyl > cyclopentadienyl. This observation is consistent with the literature report.²³ The Cent–Ru–C(cage) angles range from 111.8° to 113.0°, which

are close to the corresponding value of 112.2° found in $\text{Cp}^*\text{RuCl}(\text{COD})$.²⁴ The characteristic slippage of the indenyl and fluorenyl rings is also observed with average slip fold (Δ) values of $0.136(7) \text{ \AA}$ in **2a** and $0.142(3) \text{ \AA}$ in **3a**. All of these values can be compared with those reported in the literature.²⁵

COD Displacement Reactions. The labile nature and relative thermodynamic stability of metal-COD complexes are often used to stabilize a catalytically active organometallic fragment. The first step of the catalytic transformation involves substitution of solvent and/or substrate molecules for the outgoing COD ligand. The lability of COD ligands in $\text{LRuCl}(\text{COD})$ ($\text{L} = \text{C}_5\text{H}_5$, C_9H_7) is able to undergo exchange reactions with different tertiary phosphine ligands rapidly and quantitatively.^{24,25b,e} The COD ligand in **1a** is the most labile among the three $\text{Ru}(\text{COD})$ complexes since the π back-bonding interactions between the COD and filled d orbitals of $\text{Ru}(\text{II})$ are the weakest in **1a** as previously discussed. On the other hand, cyclopentadienyl is the smallest one among the three π ligands. Therefore, **1a** was chosen as a model complex for COD displacement reactions.

Interestingly, the COD in **1a** cannot be replaced by PR_3 ($\text{R} = \text{Ph}$, Cy) even in refluxing THF solution. This result is significantly different from $\text{LRuCl}(\text{COD})$ complexes. **1a** did not react with tertiary amines either. We then turned our attention to bidentate tertiary phosphines. Treatment of **1a** with 1.2 equiv of bidentate tertiary phosphines in THF afforded the corresponding COD displacement complexes $[\eta^5\text{-}\sigma\text{-Me}_2\text{C}(\text{C}_5\text{H}_4)\text{-(C}_2\text{B}_{10}\text{H}_{10})]\text{Ru}(\text{dppe})$ (**1b**, $\text{dppe} = 1,2\text{-bis}(\text{diphenylphosphino})\text{ethane}$), $[\eta^5\text{-}\sigma\text{-Me}_2\text{C}(\text{C}_5\text{H}_4)(\text{C}_2\text{B}_{10}\text{H}_{10})]\text{Ru}(\text{dppm})$ (**1c**, $\text{dppm} = \text{bis}(\text{diphenylphosphino})\text{methane}$), $[\eta^5\text{-}\sigma\text{-Me}_2\text{C}(\text{C}_5\text{H}_4)(\text{C}_2\text{B}_{10}\text{H}_{10})]\text{Ru}(\text{dppf})$ (**1d**, $\text{dppf} = 1,1'\text{-bis}(\text{diphenylphosphino})\text{ferrocene}$), and $[\eta^5\text{-}\sigma\text{-Me}_2\text{C}(\text{C}_5\text{H}_4)\text{-(C}_2\text{B}_{10}\text{H}_{10})]\text{Ru}(\text{dppc})$ (**1e**, $\text{dppc} = 1,2\text{-(Ph}_2\text{P)}_2\text{1,2-C}_2\text{B}_{10}\text{H}_{10}$), respectively, in 68–81% isolated yields (Scheme 3). Upon coordination, the ^{31}P NMR chemical shifts of phosphines were downfield shifted by 35–93 ppm. Therefore, these displacement reactions were well followed by the ^{31}P NMR technique.

It is noteworthy that the COD displacement reactions were irreversible; that is, **1b–e** did not react with COD to give **1a**. The ^1H and ^{31}P NMR studies indicated that only **1b** and **1a** were detected in the reaction of **1a** with 0.5 equiv of dppe , and no dinuclear species with mixed COD and dppe ligands were observed. These results may suggest that once one end (phosphine unit) of dppe coordinates to the Ru center, the other end quickly displaces the second $\text{C}=\text{C}$ bond of the COD molecule via intramolecular substitution reaction to generate the

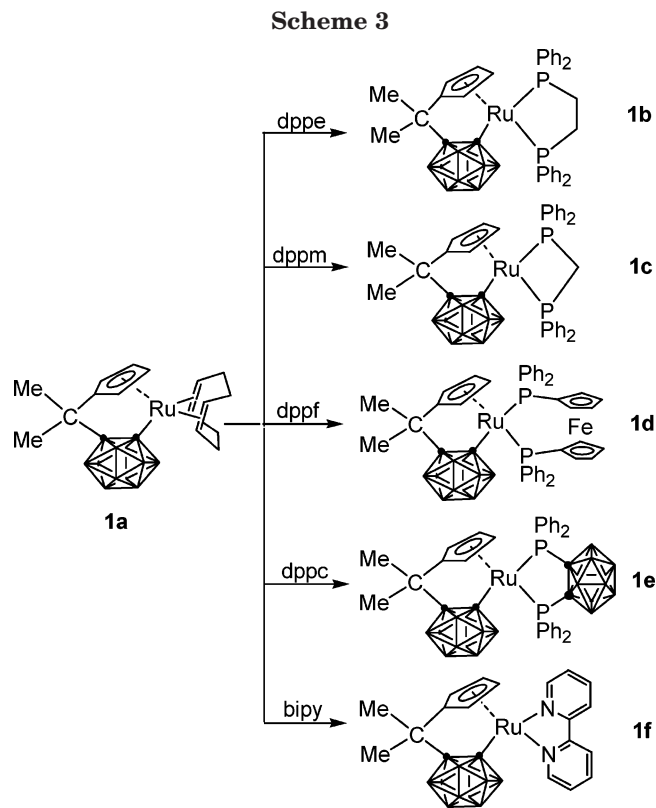


Table 4. Selected Structural Data for **1b**, **1c**, **1e**, and **1f**

	1b	1c	1e	1f
$\text{Ru}-\text{C}_{\text{cage}}$	2.141(5)	2.144(4)	2.260(4)	2.095(3)
$\text{av Ru}-\text{C}_{\text{ring}}$	2.218(7)	2.211(5)	2.237(4)	2.174(3)
$\text{av Ru}-\text{P}$	2.283(1)	2.293(1)	2.300(1)	2.067(3) ^a
$\text{P}-\text{Ru}-\text{P}$	82.08(5)	71.58(4)	87.93(3)	76.75(10) ^b
$\text{C}_{\text{ring}}-\text{C}_{\text{bridge}}-\text{C}_{\text{cage}}$	108.5(5)	108.9(4)	108.6(3)	108.9(3)
$\text{Cent}-\text{Ru}-\text{C}_{\text{cage}}$	114.3	115.0	110.0	117.8

^a Average $\text{Ru}-\text{N}$ distance. ^b $\text{N}-\text{Ru}-\text{N}$ angle.

final product **1b**, implying that the chelating effect plays a role in the COD displacement reactions. For monophosphines such as PPh_3 and PCy_3 , they may displace one of the two $\text{C}=\text{C}$ double bonds of the COD to form $[\eta^5\text{-}\sigma\text{-Me}_2\text{C}(\text{C}_5\text{H}_4)(\text{C}_2\text{B}_{10}\text{H}_{10})]\text{Ru}(\text{PR}_3)(\eta^2\text{-COD})$, which are unstable, leading to the formation of either $[\eta^5\text{-}\sigma\text{-Me}_2\text{C}(\text{C}_5\text{H}_4)(\text{C}_2\text{B}_{10}\text{H}_{10})]\text{Ru}(\eta^4\text{-COD})$ (**1a**) or $[\eta^5\text{-}\sigma\text{-Me}_2\text{C}(\text{C}_5\text{H}_4)(\text{C}_2\text{B}_{10}\text{H}_{10})]\text{Ru}(\text{PR}_3)_2$ depending on the size of incoming PR_3 molecules. The presence of a carboranyl unit in the constrained ligand not only makes the $[\eta^5\text{-}\sigma\text{-Me}_2\text{C}(\text{C}_5\text{H}_4)(\text{C}_2\text{B}_{10}\text{H}_{10})]\text{Ru}$ moiety very rigid but also reduces the open space of the central metal ion for the incoming molecule. As a result, the second PR_3 molecule cannot approach the Ru center to displace the $\eta^2\text{-COD}$. This could explain why **1a** did not react with PR_3 . Other possibilities cannot be excluded.

Complexes **1b–e** were fully characterized by various spectroscopic techniques. Only one ^{31}P resonance was observed in each complex. The pseudo- C_s symmetry of these complexes was further confirmed by single-crystal X-ray diffraction studies.

The solid-state structures of complexes **1b**, **1c**, and **1e** are shown in Figures 5–7, respectively. They have similar coordination geometries. Selected bond distances and angles are listed in Table 4 for comparison. The average $\text{Ru}-\text{C}(\text{C}_5 \text{ ring})$ and $\text{Ru}-\text{C}(\text{cage})$ distances in **1b**

(23) Gassman, P. G.; Winter, C. H. *J. Am. Chem. Soc.* **1988**, *110*, 6130.

(24) Serron, S. A.; Luo, L.; Li, C.; Cucullu, M. E.; Stevens, E. D.; Nolan, S. P. *Organometallics* **1995**, *14*, 5290.

(25) (a) Alvarez, P.; Gimeno, J.; Lastra, E.; García-Granda, S.; Van der Maalen, J. F.; Bassetti, M. *Organometallics* **2001**, *20*, 3762. (b) Li, C.; Cucullu, M. E.; McIntyre, R. A.; Stevens, E. D.; Nolan, S. P. *Organometallics* **1994**, *13*, 3621. (c) Bassetti, M.; Marini, S.; Díaz, J.; Gamasa, M. P.; Gimeno, J.; Rodríguez-Alvarez, Y.; García-Granda, S. *Organometallics* **2002**, *21*, 4815. (d) Cadierno, V.; Díez, J.; Pilar, G. M.; Gimeno, J.; Lastra, E. *Coord. Chem. Rev.* **1999**, *193–195*, 147. (e) Cucullu, M. E.; Luo, L.; Nolan, S. P.; Fagan, P. J.; Jones, N. L.; Calabrese, J. C. *Organometallics* **1995**, *14*, 289. (f) Kamigaito, M.; Watanabe, Y.; Ando, T.; Sawamoto, M. *J. Am. Chem. Soc.* **2002**, *124*, 9994.

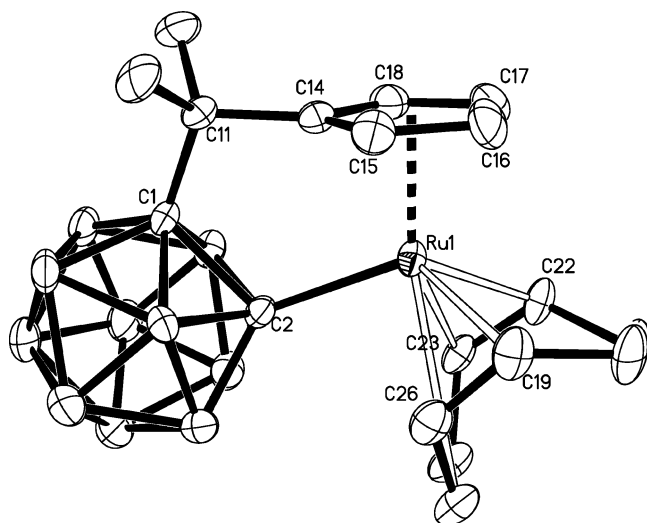


Figure 2. Molecular structure of $[\eta^5:\sigma\text{-Me}_2\text{C}(\text{C}_5\text{H}_4)\text{-(C}_2\text{B}_{10}\text{H}_{10})]\text{Ru}(\text{COD})$ (**1a**).

and **1c** are slightly shorter than those observed in **1a** and **1e**, probably due to steric reasons. The average Ru–P distances in the three complexes are very close to each other and compare well with the values reported in the literature.²⁵ The bite angles of the chelate biphosphine ligands P–Ru–P show values similar to those observed in CpRuCl(P–P) complexes.²⁵

It was reported that an increase of the bite angle of the chelating ligand results in an increase of the cone angle.²⁶ Thus the cone angles of biphosphines decrease in the order dppe > dppe > dppm. It is expected that a larger cone angle would lead to a smaller Cent–Ru–C(cage) angle, which is consistent with the experimental results shown in Table 4. The structural data in Tables 3 and 4 also indicate that the variations in the Cent–Ru–C(cage) angles observed in **1a–e** are much smaller than those found in CpRuCl(COD) and CpRuCl(P–P) complexes.²⁵ It may be concluded that the constrained geometry of the $[\eta^5:\sigma\text{-R}_2\text{C}(\text{C}_5\text{H}_4)(\text{C}_2\text{B}_{10}\text{H}_{10})]\text{Ru}$ moiety versus the flexible CpRuCl unit creates the differences in the COD displacement reactions.

Besides biphosphines, other bidentate ligands were also attempted. There were no reactions between **1a** and DME or TMEDA (DME = dimethoxyethane, TMEDA = tetramethylethylenediamine) in refluxing THF or toluene solutions. 2,2'-Bipyridine (bipy), however, was found to react with **1a** in refluxing toluene solution, affording $[\eta^5:\sigma\text{-Me}_2\text{C}(\text{C}_5\text{H}_4)(\text{C}_2\text{B}_{10}\text{H}_{10})]\text{Ru}(\eta^2\text{-bipy})$ (**1f**) as purple crystals in 68% isolated yield. It is noteworthy that pyridine did not react with **1a** under various reaction conditions. These results imply that a bidentate ligand with π -acidity is critical to displace the COD in **1a**. **1f** was fully characterized by various spectroscopic data and elemental analyses. Its structure was confirmed by a single-crystal X-ray study.

As shown in Figure 8, the Ru(II) is η^5 -bound to a cyclopentadienyl ring, σ -bound to a cage carbon atom and coordinated to two nitrogen atoms from a bipyridine molecule in a three-legged piano stool geometry. The average Ru–N bond length of 2.067(3) Å and the

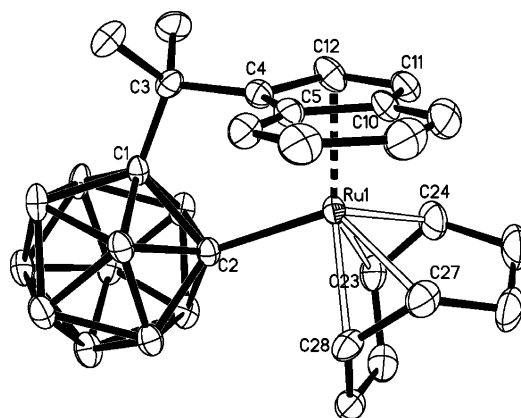


Figure 3. Molecular structure of $[\eta^5:\sigma\text{-Me}_2\text{C}(\text{C}_9\text{H}_6)\text{-(C}_2\text{B}_{10}\text{H}_{10})]\text{Ru}(\text{COD})$ (**2a**).

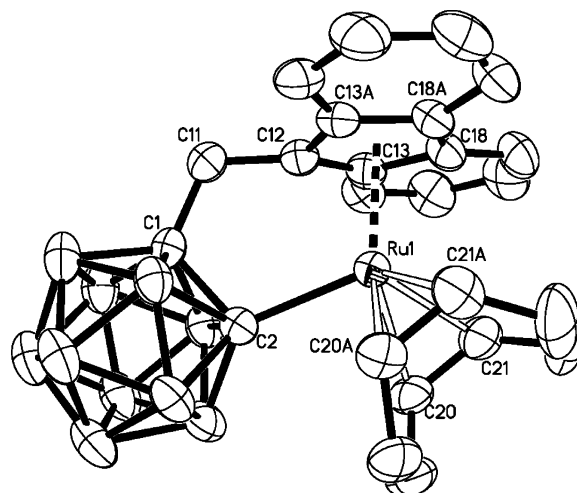


Figure 4. Molecular structure of $[\eta^5:\sigma\text{-H}_2\text{C}(\text{C}_{13}\text{H}_8)(\text{C}_2\text{B}_{10}\text{H}_{10})]\text{Ru}(\text{COD})$ (**3a**).

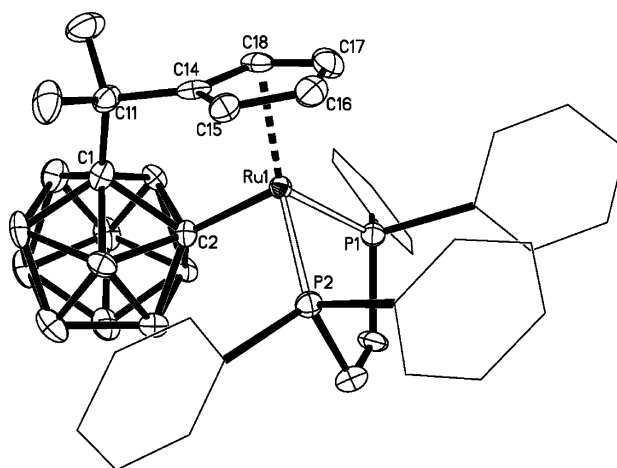


Figure 5. Molecular structure of $[\eta^5:\sigma\text{-Me}_2\text{C}(\text{C}_5\text{H}_4)\text{-(C}_2\text{B}_{10}\text{H}_{10})]\text{Ru}(\text{dppe})$ (**1b**).

N–Ru–N angle of 76.75(10)° are close to the corresponding values of 2.095(6) Å and 75.8(2)° found in $[\text{Cp}^*(\eta^2\text{-bipy})(\eta^2\text{-EtO}_2\text{C-CH=CHCO}_2\text{Et})\text{Ru}][\text{PF}_6]$.²⁷ The average Ru–C(ring) and Ru–C(cage) distances are shorter than the corresponding values observed in **1a–e**, probably owing to the relatively smaller size of bipy molecule.

(26) Van Haaren, R. J.; Goubitz, K.; Fraanje, J.; Van Strijdonck, G. P. F.; Oevering, H.; Coussens, B.; Reek, J. N. H.; Kamer, P. C. J.; Van Leeuwen, P. W. N. M. *Inorg. Chem.* **2001**, *40*, 3363.

(27) Balavoine, G. G. A.; Boyer, T.; Livage, C. *Organometallics* **1992**, *11*, 456.

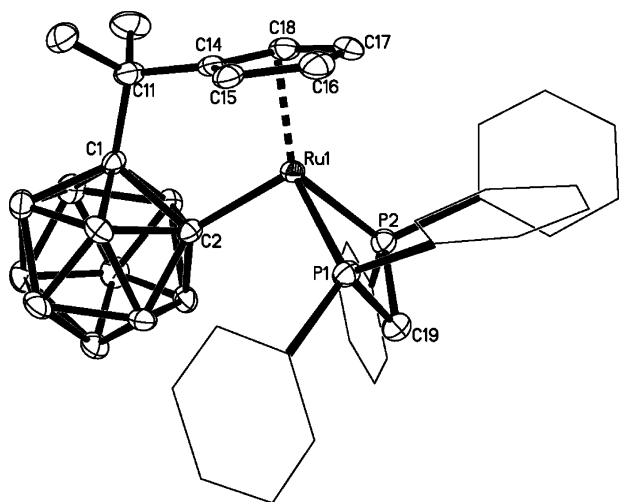


Figure 6. Molecular structure of $[\eta^5:\sigma\text{-Me}_2\text{C}(\text{C}_5\text{H}_4)\text{-(C}_2\text{B}_{10}\text{H}_{10})]\text{Ru}(\text{dppm})$ (**1c**).

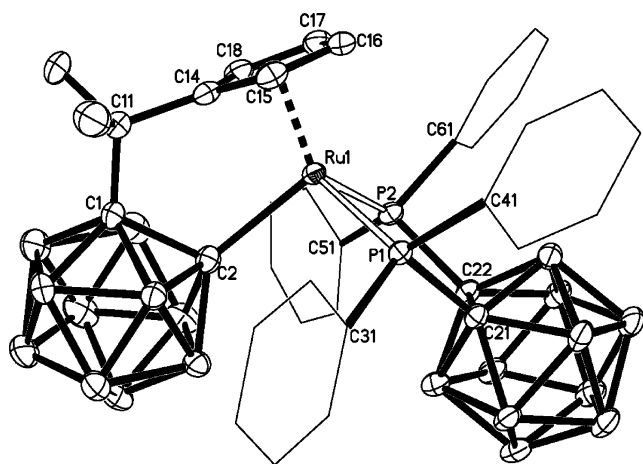


Figure 7. Molecular structure of $[\eta^5:\sigma\text{-Me}_2\text{C}(\text{C}_5\text{H}_4)\text{-(C}_2\text{B}_{10}\text{H}_{10})]\text{Ru}(\text{dppc})$ (**1e**) (the solvated THF molecule is not shown).

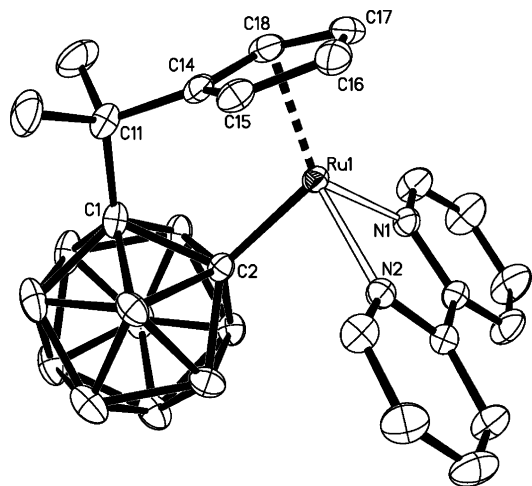


Figure 8. Molecular structure of $[\eta^5:\sigma\text{-Me}_2\text{C}(\text{C}_5\text{H}_4)\text{-(C}_2\text{B}_{10}\text{H}_{10})]\text{Ru}(\text{bipy})$ (**1f**).

Electrochemistry. For all complexes, the electrochemical study revealed that all observed redox processes are one-electron and reversible processes at the scan rate of 100 or 200 mV s^{-1} , as indicated by the ($i_{\text{pa}}/i_{\text{pc}}$) ratios of unity and the ΔE_{p} peak separations in the range 75–102 mV. The redox potentials $E_{1/2}$ given

Table 5. Redox Potentials of Ruthenium Complexes in CH_2Cl_2^a

complex	$E_{1/2}(\text{Ru}^{\text{III}}/\text{Ru}^{\text{II}})$ (V)	ΔE_{p} (mV)
1a	0.601	100
2a	0.484	91
3a	0.397 ^b	88
1b	0.250	93
1c	0.257	75
1d^c	0.659	102
1e	0.581	94
1f	−0.149	81

^a All potentials are given relative to ferrocenium/ferrocene. Pt working electrode: 100 mV s^{-1} ; recorded in CH_2Cl_2 with $n\text{-Bu}_4\text{NPF}_6$ (0.15 M) as supporting electrolyte. ^b 200 mV s^{-1} . ^c $E_{1/2}(\text{Fc}^{\text{III}}/\text{Fc}^{\text{II}}) = 0.232$ V.

relative to ferrocenium/ferrocene are compiled in Table 5. Complexes **1a**, **2a**, and **3a** have similar molecular structures with different π ligands, thus allowing us to compare the electron-donating ability of π ligands. The first three entries in Table 5 correspond to complexes **1a**, **2a**, and **3a**, indicating that the electron richness of the Ru atom increases in the order **1a** < **2a** < **3a**. This result is consistent with that previously derived from X-ray analyses and confirms that the electron-donating power of π ligands increases in the following order: cyclopentadienyl < indenyl < fluorenyl.²³ The presence of a ferrocenyl unit in **1d**, reflected by the appearance of an additional wave of the Fc^+/ Fc couple, causes a relative increase of the $\text{Ru}^{\text{III}}/\text{Ru}^{\text{II}}$ potential,²⁸ which makes it less comparable with others. Therefore, **1d** will not be compared with other Ru complexes. Thus, the electron richness of the Ru metal center increases in the order **1a** < **1e** < **2a** < **3a** < **1c** \approx **1b** < **1f**, and electron-donating abilities of the bidentate ligands follow the trend COD < dppe < dppm \approx dppe < bipy.

Conclusion

A new class of ruthenium complexes containing carbon-bridged carboranyl-cyclopentadienyl (-indenyl or -fluorenyl) ligands was synthesized and fully characterized. They are all 18-electron species and adopt a three-legged piano stool geometry. These complexes showed a different reactivity pattern in COD displacement reactions in comparison with the classical $\text{LRuCl}(\text{COD})$ ($\text{L} = \text{Cp}$, indenyl) complexes presumably due to the presence of sterically bulky and constrained organic-inorganic hybrid ligands. For example, **1a** did not react with monodentate tertiary phosphines and amines. The COD in **1a** was replaced only by bidentate ligands with π -acidity.

Both structural and electrochemical studies indicated that the electron-donating ability of π ligands increases in the order cyclopentadienyl < indenyl < fluorenyl, and the electron-donating power of σ ligands follows the trend COD < dppe < dppm \approx dppe < bipy. This work offers useful information for further investigation of this novel class of ruthenium carborane complexes for both stoichiometric and catalytic reactions.

Acknowledgment. This work was supported by grants from the Research Grants Council of The Hong Kong Special Administration Region (Project No. CUHK

4026/02P), Mainline Research Scheme of The Chinese University of Hong Kong (Project No. MR01/002), and the PROCORE–France/Hong Kong Joint Research Scheme sponsored by the Research Grants Council of Hong Kong and the Consulate General of France in Hong Kong (Reference No. F-HK15/02T). This research is also partially supported by an anonymous donor who made a donation to the Department of Chemistry at The Chinese University of Hong Kong. We thank Dr. Yaorong Wang for the preparation of complex **2a**. Z.X. acknowl-

edges the Croucher Foundation for a Senior Research Fellowship Award.

Supporting Information Available: Crystallographic data and data collection details, atomic coordinates, bond distances and angles, anisotropic thermal parameters, and hydrogen atom coordinates for **3**, **2a**, **3a**, **1a–c**, **1e**·THF, and **1f** as CIF files. This material is available free of charge via the Internet at <http://pubs.acs.org>.

OM0493816